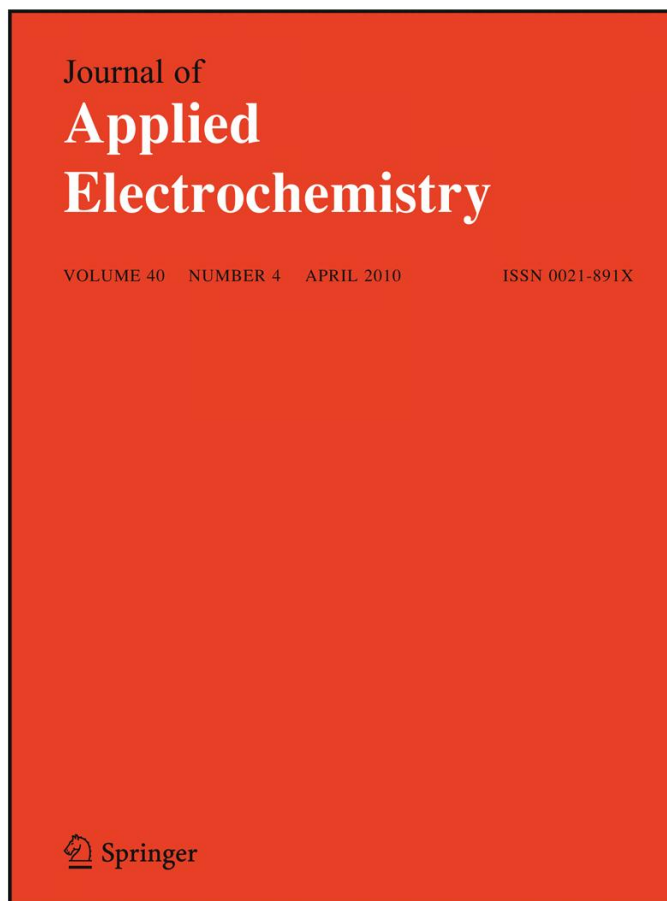


ISSN 0021-891X, Volume 40, Number 4



**This article was published in the above mentioned Springer issue.
The material, including all portions thereof, is protected by copyright;
all rights are held exclusively by Springer Science + Business Media.**

**The material is for personal use only;
commercial use is not permitted.**

**Unauthorized reproduction, transfer and/or use
may be a violation of criminal as well as civil law.**

Behavior of hydrogen nanobubbles in alkaline electrolyzed water and its rinse effect for sulfate ion remained on nickel-plated surface

Toshikazu Takenouchi

Received: 9 July 2009 / Accepted: 23 December 2009 / Published online: 14 January 2010
© Springer Science+Business Media B.V. 2010

Abstract More than ordinary rinsing using pure water, cathode water obtained by electrolysis of dilute potassium carbonate aqueous solution (alkaline electrolyzed water: AEW) exhibits a stronger rinse effect for elimination of remaining sulfate ions when rinsing nickel-plated surfaces. This rinse effect was recognized even for AEW that was used 24 h after it was produced, but not 1 week after. Behaviors of hydrogen nanobubbles observed by dynamic light scattering revealed nanobubbles of about 128-nm diameter even 24 h after generation. The Ostwald ripening phenomenon was observed. Hydrogen nanobubbles in an open system changed: some shrank because of ripening, later dissolving in the aqueous solution and disappearing; others showed swelling and expansion. One week later, few nanobubbles smaller than 300 nm were observed. Rinse effects by AEW, which are attributable to the actions of hydrogen nanobubbles generated in AEW, occur because sulfate ions are cleaned and removed from the nickel-plated surface.

Keywords Alkaline electrolyzed water · Hydrogen nanobubbles · Rinse · Sulfate ion

1 Introduction

Cathode water—obtained by electrolysis of a dilute electrolyte aqueous solution—such as alkaline electro-

lyzed water (AEW) removes particulates and surfactants from the surface of a material to be cleaned [1]. It has cleaning performance that is comparable to a degreasing or cleaning method using conventional chemicals, rendering it useful for precision cleaning [2]. The electrolyzed water has high alkalinity. Moreover, hydrogen bubbles resulting from electrolysis act on the material to be cleaned and the particulates that are present on its surface, thereby improving the cleaning effects. In the semiconductor field, hydrogen-dissolved water (hydrogen gas dissolved in ultrapure water) is used to remove nonionic particulates from silicon wafer surfaces and is used in practical wafer cleaning processes [3]. Ultrasonic irradiation of hydrogen-dissolved water reportedly enhances particulate removal effects by virtue of the fine hydrogen bubbles generated by the ultrasonic waves [4].

The authors, considering that AEW might remove ionic impurities in addition to degreasing, cleaning, and particulate removal effects, have been promoting its investigation. Empirically, it is known that a Watts bath, primarily using nickel sulfate, leaves sulfate ions on a nickel-plated surface to be cleaned. For removal of ionic impurities including sulfate ions, various techniques are used during cleaning after plating: repeated cleaning with pure water, ultrasonic cleaning, or the like. In a previous article, we reported that cleaning with pure water after a nickel-plated specimen was once immersed into AEW (hereinafter, rinsing) was able to decrease the amount of sulfate ions remaining on the nickel-plated surface [5]. Results of this study verified our idea that the rinse effects of AEW are attributable to hydrogen bubbles generated in AEW, particularly nanosize hydrogen bubbles (hereinafter, hydrogen nanobubbles).

T. Takenouchi (✉)
Research and Development Division, Shinko Electric Industries
Co., Ltd, 36 Kitaowaribe, Nagano-shi 381-0014, Japan
e-mail: ttakenoh@shinko.co.jp

2 Experimental

2.1 Reagents, conditions, and apparatus for AEW generation

Potassium carbonate (analytical reagent grade; Wako Pure Chemical Industries Ltd.) was used as the electrolyte for AEW generation, along with an electrolytic apparatus (Espax; Zipcom Co. Ltd.) used for maintaining the concentration of potassium carbonate in aqueous solution at 0.01 wt%. Pure water having resistivity of more than 10 M Ω cm was generated using ion exchange and reverse osmosis, and passed through a filter having openings of 0.1 μ m. The electrolytic apparatus we used is a continuous-generating-type cylindrical electrolytic compartment consisting of a diaphragm with a neutral membrane filter (Yumicon; GS Yuasa Battery Ltd.) and platinum-coated titanium electrodes (plating thickness 1 μ m; Tanaka Kikinokoku Group). The anode and cathode electrode apparent surface areas were, respectively, 922 and 1,063 cm². Electrolytic conditions were 50 V voltage, 15 A current, and a 3 dm³ min⁻¹ flow rate. Figure 1 shows the electrolytic cell. Measurements of the aqueous solution's pH, redox potential, and concentration of dissolved hydrogen were conducted, respectively, using a pH meter (F-22; Horiba Instruments Ltd.), a redox potential meter (TRX-90; Toko Kagaku Co. Ltd.), and a dissolved hydrogen meter (DH-35A; DKK-TOA Corp.).

2.2 Rinse effect experiments by AEW

Experiments were performed according to the following steps to verify that AEW rinses away sulfate ions [5]:

- (1) A copper substrate (20 mm \times 20 mm \times 1 mm) was nickel-plated electrolytically using a Watts bath to yield 1 μ m thickness.

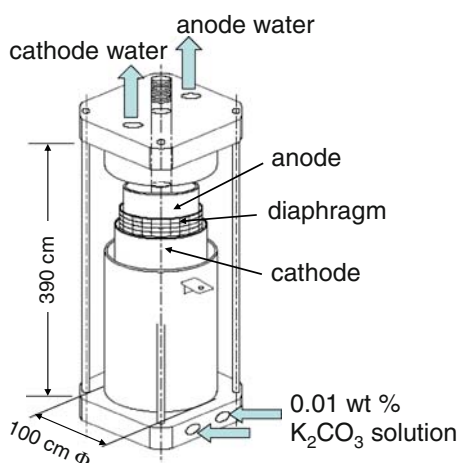


Fig. 1 Schematic diagram of electrolytic cell

- (2) The specimen was immersed into AEW with 0.5 dm³, dipped in and out in a vertically oscillating fashion three times, and immersed for a total of 3 s (rinsing by AEW). Because of the comparative control, the same operations were performed using pure water instead of AEW.
- (3) Pure water was introduced at a rate of 2 dm³ min⁻¹; the specimen was cleaned with this running water for a minute.
- (4) Dry nitrogen gas was blown on the specimen for drying.
- (5) The specimen was boiled in ultrapure water. Then concentrations of anion and cations contained in the boiling water were determined using ion chromatography (DX-120; Dionex Corp.) based on JIS K0556. The amount of ionic impurities per unit area of the specimen was obtained. Ultrapure water with resistivity of not less than 18 M Ω cm was used. Experiments were performed three times; their values were averaged and used for analyses.

The experiments described above were performed using AEW immediately after generation, AEW 24 h after generation, and AEW 1 week after generation. The results were compared. Then AEW was stored at room temperature in open conditions.

2.3 Measurements of hydrogen nanobubbles

A dynamic light scattering photometer (FDLS-3000; Otsuka Electronics Co. Ltd.) was used for particle diameter and size distribution measurements of the hydrogen bubbles in AEW. This study used a dynamic light scattering apparatus with a light source equipped with a semiconductor excitation solid-state laser having 523 nm wavelength [6]. The use of wavelengths shorter than the conventional 780 nm improved the detection sensitivity by 50–100 times. The hydrogen nanobubble behaviors were therefore more clearly identifiable. Dynamic light scattering measurements were conducted for AEW preserved for 5 h, 24 h, and 1 week after preparation. In the closed system, the AEW was left in the dark in a stoppered flask with no headspace. In the open system, it was left in a non-stoppered flask at room temperature. The closed system specimen was used after storage for 5 h.

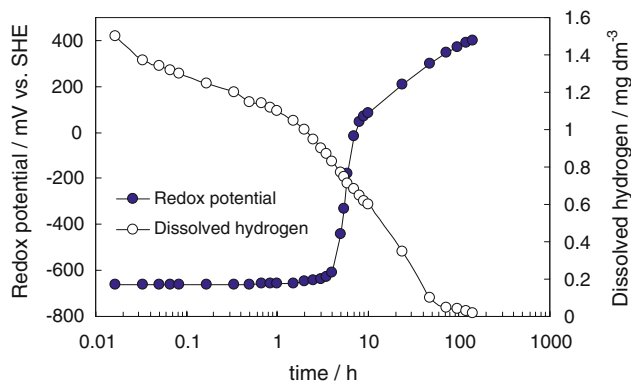
3 Results and discussion

3.1 Characteristics of AEW

Table 1 portrays characteristics of AEW of potassium carbonate. The redox potential of AEW was remarkably

Table 1 Characteristics of AEW and 0.01 wt% K_2CO_3 aqueous solution

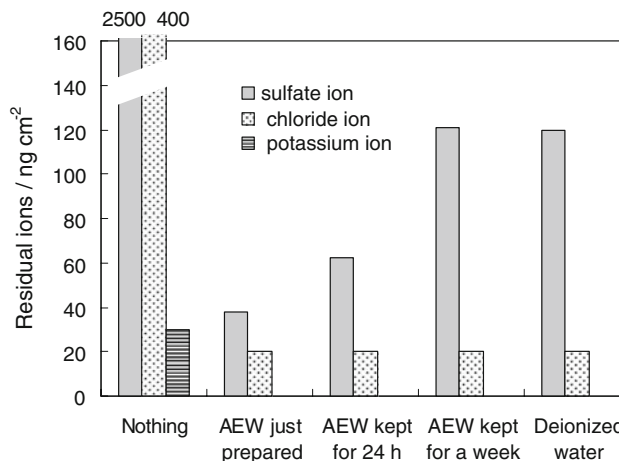
| | AEW | 0.01 wt% K_2CO_3 solution |
|---|-------|-----------------------------|
| pH | 11.90 | 10.50 |
| Redox potential ^a /mV versus SHE | −690 | 370 |
| Dissolved hydrogen ^a /mg dm^{-3} | 1.20 | 0.00 |

^a Measured in 5 min after electrolysis**Fig. 2** Change in redox potential and dissolved hydrogen concentration of AEW of 0.01 wt% K_2CO_3 with elapsed time after electrolysis

lower and the dissolved hydrogen concentration was higher than that of the aqueous solution of potassium carbonate, which was not subjected to electrolysis. According to the Nernst equation, the pH and hydrogen generation potential are expressed as $E_H = -RT/2F \ln P_{H_2} - 0.059 \text{ pH}$. At 25 °C and atmospheric pressure, it is expressed as $E_H = -0.059 \text{ pH}$; results of the measurement nearly satisfied the relational expression. Furthermore, Figure 2 portrays temporal changes in the redox potential of AEW and the concentration of dissolved hydrogen. Figure 2 shows that although a slight change in redox potential is noticed until 4 h after generation, it increases rapidly at 5–6 h and thereafter. The reduced concentration of dissolved hydrogen causes this change.

3.2 Amount of sulfate ions remaining on the surface of specimen

The amount of sulfate ions remaining on the surface of the specimen is depicted in Fig. 3. The quantitative limit of sulfate ions shown by ion chromatography is $0.1 \mu\text{g } dm^{-3}$. The sulfate ions remaining on the specimen surface immediately after plating were $2,500 \text{ ng } cm^{-2}$. That value was $40 \text{ ng } cm^{-2}$ after cleaning by rinsing with AEW and subsequent rinsing with pure water. It was $120 \text{ ng } cm^{-2}$ when pure water was used for rinsing. Although sulfate ions are liable to remain for cases in which all cleaning

**Fig. 3** Amount of residual ions on electroplated nickel specimen rinsed with AEW. Specimen was treated nothing, rinsed with AEW just prepared, AEW kept for 24 h, AEW kept for a week, and deionized water only

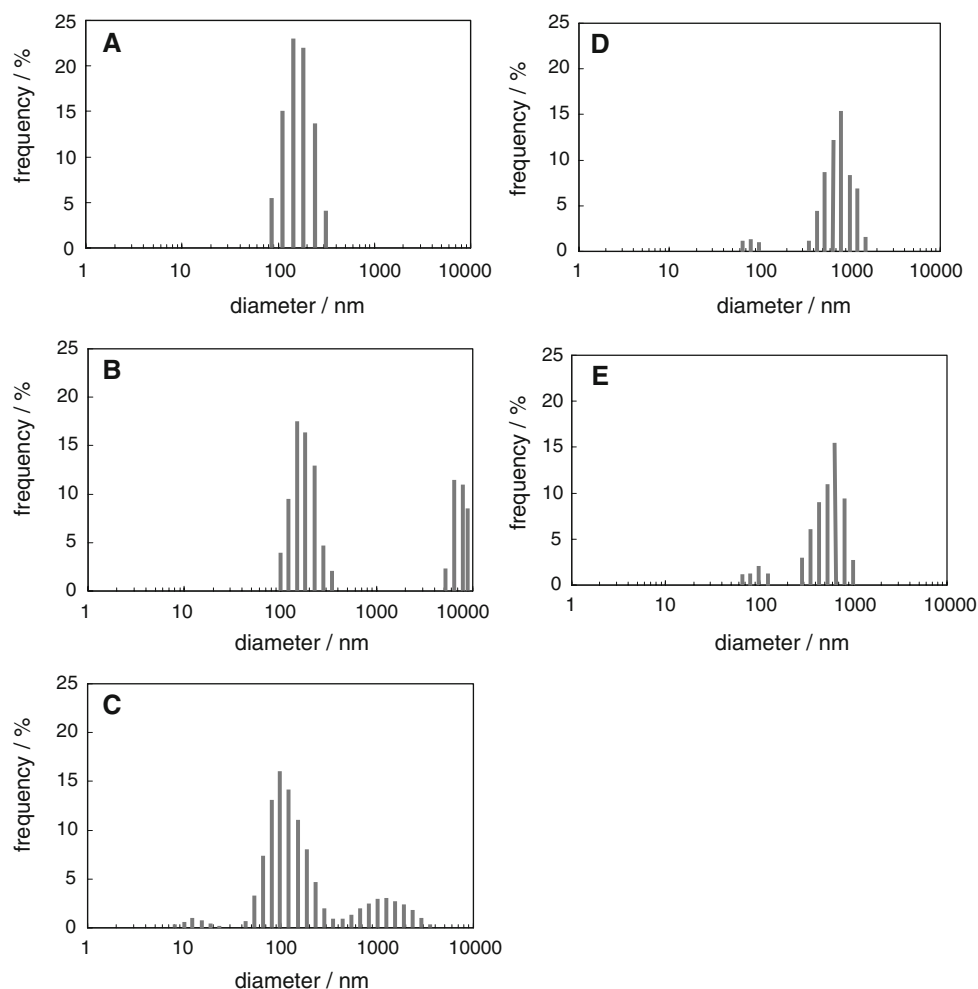
after plating is performed with pure water, when rinsing with AEW was performed, fewer sulfate ions adhered, thereby exhibiting the rinse effect. The result of similar experiments using materials 24 h after AEW generation was $60 \text{ ng } cm^{-2}$. However, the use of AEW 1 week after generation yielded identical results to those obtained when the surface had been cleaned solely with pure water. This phenomenon is likely to be associated with the hydrogen nanobubbles in AEW, as described later. For chloride ions, no difference was found in either case. Although the remaining sulfate ions were fewer—although chloride ions are rinsed more easily than sulfate ions—some infinitesimal amount of the ions invariably remains. Existing potassium ion amounts were originally small and were not detected after rinsing.

Takahashi [7] identified that air nanobubbles in the water are stable for a long period. Similarly, it is considered that hydrogen nanobubbles exist stably for a long period. The fact that the rinse effect appeared even 24 h after AEW generation suggests that hydrogen nanobubbles exist in a stable manner. However, the rinse effect disappears within AEW 1 week after its generation, implying that hydrogen nanobubbles contributing to the rinse effect had disappeared.

3.3 Behavior of hydrogen nanobubbles in AEW

Regarding water electrolysis, water molecules are reduced, producing hydrogen molecules on the electrode surface. Hydrogen bubbles are generated from the hydrogen molecules. The hydrogen bubbles then combine to produce hydrogen nanobubbles. Therefore, most nanobubbles are of hydrogen.

Fig. 4 Distribution of hydrogen bubble sizes in AEW. Measured after electrolysis; **a**: 5 h, closed system, average size (ave.) 160 nm, **b**: 24 h, closed system, ave. 184 nm, **c**: 24 h, open system, ave. 13, 128, and 1349 nm, **d**: 1 week, closed system, ave. 750 nm, **e**: 1 week, open system, ave. 735 nm



The particle size distribution of hydrogen nanobubbles in the closed system 5 h after AEW generation is portrayed in Fig. 4a. The average particle diameter was 160 nm. The dissolved hydrogen concentration was 1.20 mg dm^{-3} . Figure 4b presents the distribution in the closed system 24 h later: the particle size distribution was 100–300 nm; the average particle diameter was 184 nm; and the dissolved hydrogen concentration was 0.98 mg dm^{-3} . At the same time, 5–10 μm microbubbles were also generated, probably because of generation of micrometer-size bubbles as a result of binding of some hydrogen nanobubbles. In the closed system, nanobubbles grew slightly and were stable, although the dissolved hydrogen concentration decreased slightly. Figure 4c portrays the distribution in the open system observed 24 h later. Three peaks were observed: their average particle diameters were, respectively, 13, 128, and 1349 nm. This phenomenon illustrates Ostwald ripening. Regarding hydrogen nanobubbles' changes in particle diameter in the open system, some shrank because of ripening, dissolving in the aqueous solution and disappearing, but others expanded [6]. The dissolved hydrogen

concentration was 0.30 mg dm^{-3} . Figure 4d presents the distribution in the closed system 1 week later. Nanobubbles of around 184 nm, as shown in Fig. 4b (24 h after, closed system) had almost disappeared. The distribution in 350–1,500 nm (average particle diameter 750 nm) increased. Figure 4e depicts the distribution in the open system 1 week later. Nanobubbles of around 128 nm, as observed in C (24 h after, open system), were very few. The distribution of bubbles of 300–1,200 nm particle diameter (average 735 nm) increased. It is readily apparent from Fig. 4 that the frequency of hydrogen nanobubbles 24 h later is 30–40% less than that 5 h later. The sulfate ions remaining for AEW kept for 24 h were 1.5 times more numerous than those in AEW that had just been prepared (Fig. 3). Based on this result, the presence of hydrogen nanobubbles is inferred to cause rinse effects.

Kikuchi et al. identified that, for hydrogen in AEW, dissolved hydrogen is dissolved in molecular form at more than the saturated concentration. Furthermore, fine hydrogen bubbles (hydrogen nanobubbles) coexist in colloidal form [8]. In their experimental conditions, hydrogen

nanobubbles disappeared in 3 h. Additionally, its stability depends on the current density and ionic strength [9]. In this study, experiments were conducted under higher current density and lower electrolyte concentration conditions than the electrolysis conditions used in the study by Kikuchi et al. Therefore, we presume that hydrogen nanobubbles are likely to exist more stably than in the case investigated by Kikuchi et al. The reason for the stable presence of hydrogen nanobubbles remains unknown, but elucidation of this mechanism is an important future task.

The experiments described herein demonstrated that hydrogen nanobubbles in AEW exist even 24 h later in closed systems at sizes of 100–300 nm. They shrink in open systems and have a distribution peak around 128 nm. The nanobubbles exist in stable fashion in either case. Their rinse effects are reasonably explainable considering that the action of nanobubbles smaller than 300 nm is associated with cleaning action by AEW.

Previously, the authors measured hydrogen bubbles that were present in AEW and their particle size distribution using dynamic light scattering with a storage type electrolytic apparatus. Consequently, hydrogen bubbles of micrometer and nanometer size were observed. Hydrogen bubbles mutually join over time to become large bubbles; they then flow outside the liquid and disappear in about 1 h [5]. Although the stability of hydrogen bubbles depends on electrolytic conditions and the electrolyte type, fine hydrogen bubbles reportedly disappear in about 1–6 h [10]. Therefore, AEW should be used immediately after its generation. Although optimization of electrolytic conditions for the stable existence of hydrogen nanobubbles in AEW is difficult, the specifications used for this study supported storage of AEW containing hydrogen nanobubbles in a comparatively stable fashion for up to about 24 h.

3.4 Rinse effect of AEW for sulfate ions

Regarding the mechanism of particle removal from a silicon wafer using hydrogen-dissolved water, it is considered that (i) hydrogen bubbles in the aqueous solution adhere to the particulates and act as a physical peeling force, lifting them off the silicon wafer, and that (ii) hydrogen radicals bond to the uppermost surface of the wafer and render the surface inactive [4]. Moreover, because the zeta-potential on the surfaces of silicon wafer and particulates have higher negative zeta-potential in the alkaline aqueous solution, the removed particulates repel each other by electric repulsion force, repelling the silicon wafer also. Therefore, they do not mutually readhere [11]. This concept is derived from Lange's theory [12]. The rinse effect by AEW can also be considered as attributable to actions by hydrogen bubbles similarly to the mechanism for particulate removal. Previously, the authors demonstrated that AEW is an aqueous

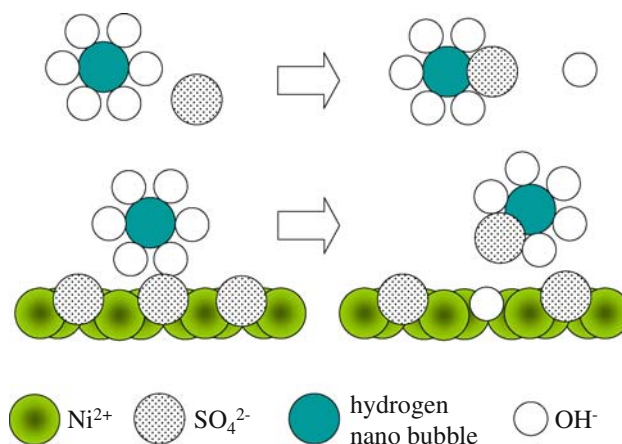


Fig. 5 Schematic diagram of sulfate ions removal by hydrogen nanobubbles in AEW

solution having negative zeta-potential including nanosize and micrometer-size hydrogen bubbles [5]. Therefore, hydrogen generated from electrolysis is present in AEW as negatively charged colloidal bubbles. Hydroxide ions are reportedly adsorbed onto the surface of negatively charged hydrogen bubbles [9]. Air nanobubbles also have higher negative zeta-potential, and hydroxide ions gather on a sliding plane of electric double layer at the interface between air nanobubbles and water [7]. Presumably, when a nickel-plated surface is rinsed with AEW, selective replacement reactions attributable to the ion exchange reaction between hydroxide ions being adsorbed onto the surface of hydrogen nanobubbles occur, along with sulfate ions being adsorbed onto the nickel surface. Consequently, sulfate ions on the nickel surface are desorbed. Desorbed sulfate ions do not readhere onto the nickel surface, probably because of repulsion with similarly negatively charged hydrogen nanobubbles. They are therefore rinsed efficiently. The material to be cleaned is eventually purified. Figure 5 shows an estimated model of this replacement reaction.

According to the Pourbaix diagram [13], nickel is positioned in the corrosive region when in a strong alkaline solution. However, measurements of nickel soaked in AEW for 1 month and nickel ion concentration in the aqueous solution detected no nickel ions. Apparently, AEW dissolves nickel only slightly. In other words, dissolution of the nickel uppermost surface does not eliminate sulfate ions. Desorption eliminates the ions through interaction with hydrogen nanobubbles.

3.5 Specific adsorption of sulfate ions

Sulfate ions are known to adhere to nickel-plated layer surfaces. Even rinsing with pure water does not remove them easily. A silicon wafer cleaned using a sulfuric acid/

hydrogen peroxide mixture showed a similar phenomenon. Reportedly, the complete removal of the sulfate ions remaining on the wafer is extremely difficult using ultra-pure water alone [14, 15]. To date, the specific adsorption of sulfate ions on the electrode surface remains unclear. Results of recent studies show that sulfate ions specifically adsorb onto the surfaces of some metals and influence subsequent crystal growth. Results of analyses conducted at a large radiation facility (Super Photon ring 8 GeV; Spring-8) indicate that oxygen atoms of the sulfate ions form a closely packed structure surrounding the copper (I) ions. The distance between the two oxygen atoms is comparable to that of the hydrogen bond in the plane of the closely packed oxygen atoms when copper is deposited on a gold electrode using a copper sulfate aqueous solution [16]. In that study, the sulfate ions adsorbed to Cu under potential deposition (UPD) and were deposited on a Au(111) electrode in a sulfuric acid aqueous solution [17]. The specific adsorption of the sulfate ions on an Ir(111) electrode was also observed [18]. Consequently, although the sulfate ions had not been considered previously as a chemical species that easily underwent specific adsorption, the phenomenon by which the sulfate ions were specifically adsorbed onto an electrode showed a significant influence. These results imply that sulfate ions are adsorbed easily onto the nickel-plated surface. Presumably, during nickel deposition, the nickel ions deposit in the structure surrounded by the oxygen atoms of the sulfate ions. Then the sulfate ions, retaining covalent bonds, are adsorbed onto the nickel surface. They cannot be removed easily by subsequent cleaning treatment.

4 Conclusion

The authors have inferred that rinse effects of sulfate ions remaining on the nickel-plated surface by AEW are attributable to the hydrogen nanobubbles in AEW. We measured the particle diameter and size distribution of hydrogen nanobubbles in AEW using dynamic light scattering and explored possible relations between their behaviors and the rinse effects. The following findings were obtained.

(1) Actually, AEW, when used for cleaning of the nickel-plated surface, has a rinse effect that is better capable of reducing the amount of remaining sulfate ions than cleaning with pure water alone. This rinse effect was confirmed for AEW even 24 h after generation. No rinse effect was noticed with AEW 1 week after generation.

- (2) Confirmation of hydrogen nanobubbles in AEW using dynamic light scattering revealed that nanobubbles of about 128 nm diameter were present in a stable fashion even 24 h after their generation. However, 1 week later, few nanobubbles smaller than 300 nm diameter were observed.
- (3) The authors consider that a rinse effect occurs because of hydrogen nanobubbles generated in AEW. The AEW cleans and removes sulfate ions efficiently from the nickel-plated surface because sulfate ions replace hydroxide ions on the hydrogen nanobubble surfaces. The sulfate ions are adsorbed selectively onto the hydrogen nanobubble surfaces.

Acknowledgments The authors wish to thank Mr. Mitsuki Hashimoto and Mr. Kazushi Sasa of Otsuka Electronics Co. Ltd. for their assistance with measurement of the particle size and size distribution of hydrogen nanobubbles. We also wish to thank Dr. Shinichi Wakabayashi of the Nagano Techno Foundation for his valuable advice related to the specific adsorption of sulfate ions.

References

1. Furuguchi T, Morishita A (2002) Japan Patent Application No. 2002-155006
2. Takenouchi T, Tanaka H, Wakabayashi S (2003) *J Surf Finish Soc Jpn* 54:818
3. Imaoka T, Yamanaka K (2000) *J Surf Finish Soc Jpn* 51:141
4. Morita H, Ida J, Ota O, Tsukamoto K, Ohmi T (2001) *Solid State Phenom* 76–77:245–250
5. Takenouchi T, Wakabayashi S (2006) *J Appl Electrochem* 36:1127
6. Takenouchi T, Sato U, Nishio Y (2009) *Electrochemistry* 77:521
7. Takahashi M (2005) *J Phys Chem B* 109:21858
8. Kikuchi K, Takeda H, Rabolt B, Okaya T, Ogumi Z, Saihara Y, Noguchi H (2001) *J Electroanal Chem* 506:22
9. Kikuchi K, Tanana Y, Saihara Y, Maeda M, Kawamura M, Ogumi Z (2006) *Colloid Interface Sci* 298:914
10. Kikuchi K (2004) *The characteristics and advanced technology of water*. NTS, Tokyo, p 24
11. Morinaga H (2001) *Jpn Soc Appl Phys* 70:1067
12. Ohki K, Yagi K (1993) *Basic knowledge of cleaning*. Sangyo-Tosyo, Tokyo, p 28
13. Pourbaix M (1974) *Atlas of electrochemical equilibria in aqueous solutions*. National Association of Corrosion Engineers, Houston
14. Yamasaki S, Aoki H, Nishiyama I, Aoto H (1997) *Proc. of Jpn Soc Appl Physics annual meeting 1997 spring*, Tokyo, p 775
15. Yamanaka K, Futatsuki T, Aoki H, Nakamori M, Aoto N (1996) *Proc. of 5th international symposium on semiconductor manufacturing*, Tokyo, p 200
16. Nakamura M, Endo O, Ohta T, Ito M, Yoda Y (2002) *Surf Sci* 514:227
17. Seo M (2007) *J Surf Finish Soc Jpn* 58:655
18. Wan LJ, Hara M, Inukai J, Itaya K (1999) *J Phys Chem B* 103:6978